Available online at www.CivileJournal.org

Civil Engineering Journal

(E-ISSN: 2476-3055; ISSN: 2676-6957)

Vol. 11, No. 09, September, 2025

Subsurface Mapping and Geotechnical Design for Landslide Mitigation

Muhammad Fathur Rouf Hasan [1, 2], Adi Susilo [2, 3*], Alexander T. Sutan Haji [4], Eko Andi Suryo [2, 5], P. A. Maha Agung [6], Mohammad Habibiy Idmi [3], Baba Musta [7]

[1] *Graduate School, Universitas Brawijaya, Malang, 65145, Indonesia.*

[2] *Center Study on Geosciences and Hazard Mitigation, Universitas Brawijaya, Malang, 65145, Indonesia.*

[3] *Department of Physic, Faculty of Mathematics and Natural Sciences, Universitas Brawijaya, Malang, 65145, Indonesia.*

[4] *Department of Biosystem Engineering, Faculty of Agricultural Technology, Universitas Brawijaya, 65145, Indonesia.*

[5] *Department of Civil Engineering, Faculty of Engineering, Universitas Brawijaya, 65145, Indonesia.*

[6] *Department of Civil Engineering, Politeknik Negeri Jakarta, Depok, 16425, Indonesia.*

[7] *Geology Program, Faculty of Science and Technology, Universiti Malaysia Sabah, Sabah, 88400, Malaysia.*

Received 22 April 2025; Revised 09 August 2025; Accepted 16 August 2025; Published 01 September 2025

Abstract

The landslide near the PT Molindo Incinerator Unit poses a significant threat to the facility's structural integrity. Without immediate mitigation measures, the incinerator building is at risk of collapse, potentially impacting adjacent settlements due to cascading structural failures. To reduce the risk of further instability, urgent geophysical investigation is required to characterize the subsurface lithology and assess the groundwater table conditions. A geoelectrical resistivity survey was conducted using the Schlumberger configuration across 8 measurement points along a 100-meter survey line, with 10-meter electrode spacing. The resistivity measurements ranged from 3.30 to 25 Ωm, which were interpreted as clay-rich layers; 26 to 167 Ωm, corresponding to sandy clay; and 167 to 15,944 Ωm, indicating bedrock. The potential slip zone is interpreted at an average depth of 20 to 25 meters, indicated by very low resistivity values with resistivity values between 3.30 and 25 Ωm. Field observations confirmed that the landslide materials predominantly consisted of clay soils, distributed within two distinct layers beneath the incinerator unit. The combined depth of the clay and overlying sandy layers was estimated to reach approximately 20-25 meters from the ground surface. To ensure the effectiveness of structural mitigation, a retaining wall must be designed to extend beyond this depth threshold. Numerical simulations using Slope/W software indicated that soil nailing techniques yielded safety factors ranging from 1.32 to 1.81 under static conditions and 1.22 to 1.43 under dynamic conditions. Predicted deformations ranged from 0.01 to 0.02 meters (static) and 0.02 to 0.03 meters (dynamic). These results suggest that soil nailing is a viable reinforcement method to stabilize slope movements, particularly during periods of high rainfall. Additional recommended mitigation strategies include the installation of surface and subsurface drainage systems to control water flow, constructing retaining structures to serve as physical barriers to soil movement, and using vegetative cover to enhance slope stability.

Keywords: Clay Soil; Geotechnical Design; Landslide; Mitigation; Resistivity Survey.

1. Introduction

Landslides are geological hazards involving the downslope movement of rock masses or soil, which may occur in various forms such as rockfalls, debris flows, or large-scale soil displacements. Landslides are natural disasters caused

* Corresponding author: adisusilo@ub.ac.id

http://dx.doi.org/10.28991/CEJ-2025-011-09-015

by natural or human factors; these disasters can cause detrimental impacts such as infrastructure damage, economic losses, and the most fatal is the loss of human life [1, 2]. Landslides are prevalent globally in mountainous and high-relief regions [3]. In Indonesia, common triggering factors include steep terrain, seismic activity, and extreme weather conditions, with rainfall-induced landslides being the most frequent. Topographic features, especially slopes, increase susceptibility during periods of intense precipitation [4]. One of the most landslide-prone regions in Indonesia is Malang Regency, located in East Java. Surrounded by mountainous terrain with varying slope gradients, the area consistently exhibits a high risk of slope instability. According to data from the Malang Regency Regional Disaster Management Agency (BPBD), 333 landslide incidents were recorded between 2017 and July 2022, a five-and-a-half-year period [5]. [5]. Of the 33 districts in the regency, 17 have experienced recurring landslides, indicating that approximately 50% of the area is highly susceptible.

Generally, rainfall is the main factor triggering landslides [6], such as the landslide incident that occurred near the limited liability company (PT) A recent landslide near the PT Molindo Lawang Incinerator Unit was triggered by extreme rainfall on March 8, 2022. Over 100 mm of rainfall fell within a few hours, significantly elevating the groundwater level and saturating the clay-dominated soil profile [7]. Water infiltration into the clay matrix led to expansion and a reduction in interparticle cohesion. As the frictional resistance within the soil mass decreased, approaching a near-zero static friction coefficient, the slope failed, initiating a landslide. A comprehensive understanding of the subsurface conditions is essential to mitigate further slope failure and assess the extent of instability. This includes delineating rock layers and groundwater characteristics [8], which serve as a foundation for geotechnical engineering designs [9]. Landslide susceptibility maps and subsurface investigations are valuable tools for informing engineers, planners, local authorities, and communities about appropriate construction, zoning, and risk management strategies in affected areas [10].

Although landslides cannot be entirely prevented, their impacts can be minimized through appropriate mitigation strategies [4, 11]. With the high risk of recurrence in the PT Molindo area, further subsurface investigations are warranted to inform appropriate engineering responses [12]. One effective method is geoelectrical resistivity surveying [13], which has been widely employed in landslide studies worldwide in recent decades. Technically, the effective resistivity geoelectric method is used to evaluate the thickness of the soft clay layer in the failure zone [14]. Several studies using the geoelectrical resistivity method for landslide investigations have been carried out; Di Maio et al. (2024) correlated geotechnical and geophysical methods for monitoring soil hydrology on soil-mantled slopes prone to landslides. The results showed that electrical resistivity is closely correlated with volumetric water content and soil water pressure, thus making resistivity a potential indicator of soil hydrological status at the slope scale [15]. Hasan et al. (2024) used the geoelectric resistivity method to determine the position of the slip zone on the road connecting Batu City, Malang Regency, and Kediri Regency; the results showed that the slip zone was found at a depth of 25 meters [16]. Sujitapan et al. (2024) collaborated on geoelectric and seismic methods to investigate landslides in southern Thailand. They succeeded in mapping the slip zone at a depth of less than 5 m and estimated the volume of landslide material at around 33,447 m³ [17]. Generally, previous studies have been limited to determining the position of the slip zone. The difference between this study and previous studies is that this study investigates the landslide area using the geoelectric resistivity method, along with design recommendations for post-landslide management and reducing the potential for subsequent landslides.

Resistivity methods are commonly used in landslide investigations to distinguish surface soil from bedrock, determine the types of rock layers, their thickness, and the depth of their lithological composition [8]. Once the subsurface lithology and groundwater conditions are established, numerical modeling and geotechnical design, such as the planning of retaining walls and deep foundation elements, can be undertaken. These measures must be carefully designed to anchor into competent strata and ensure long-term slope stability. This study aims to investigate the subsurface geological conditions at the PT Molindo landslide site as a basis for developing an effective geotechnical mitigation plan and slope stabilization design. This study presents a subsurface investigation using the geoelectrical resistivity method in a post-landslide area. The investigation results serve as the basis for developing recommendations for landslide impact management, aimed at formulating mitigation strategies and reducing the potential for subsequent landslides.

2. Methodology

2.1. Resistivity Survey

The geoelectrical resistivity method is a geophysical technique used to determine variations in rock resistivity by measuring the potential difference generated by an injected artificial current. The resistivity values are influenced by mineral composition, water content, and the degree of fluid saturation, making this method effective for investigating saturated zones and slip zone areas. The Schlumberger configuration of the geoelectrical resistivity survey incorporates Vertical Electrical Sounding (VES) techniques, whereby the resistivity of subsurface rock layers is measured along a vertical profile. The use of the Schlumberger configuration is more advantageous for landslide investigations, as it provides better depth resolution and results, while offering a measurement technique that is relatively easy to apply in difficult terrains, such as post-landslide areas. The resistivity method operates by injecting an electric current into the ground through a pair of current electrodes, while the resulting potential difference is measured using a separate pair of potential electrodes [18].

As illustrated in Figure 1, the Schlumberger configuration utilizes four electrodes: two outer electrodes (A and B) for current injection and two inner electrodes (M and N) for potential measurement [19]. In this arrangement, the spacing between the potential electrodes (MN) is maintained at a constant 2 meters, while the spacing between the current electrodes (AB) is progressively increased from 10 meters and its multiples, extending to 200 meters. Expanding the AB spacing allows the injected current to penetrate deeper into the subsurface, following the principle that the MN/2 distance must remain significantly smaller than AB/2 to maintain measurement accuracy. The measured data is then calculated using Microsoft Excel to determine the geometric factor (K) and subsequently the apparent resistivity (ρ_a). The (ρ_a) was calculated as the product of the geometric factor (K) and the measured resistance (R) using Equation 1:

$$\rho_a = K\frac{\Delta V}{I} \tag{1}$$

where, (ΔV) is measurable potential difference value and (I) is electric current injected value. The results of the apparent resistivity measurements are plotted as a function of the current electrode distance (AB/2), then interpreted through an inversion process to obtain the actual resistivity model. Measurement results are processed using software such as IPI2Win and Progress to obtain 1D model and Surfer to obtain 2D model [20]. Combining individual VES measurements can generate a two-dimensional cross-section using a pseudo-cross-section model in Surfer software, which integrates parameters such as resistivity, survey track length, and depth [20]. This approach effectively transforms one-dimensional data into a two-dimensional representation by interpolating between adjacent VES points by constructing straight-line segments connecting them. The modeling results are then interpreted with geological maps and information obtained from the field. This research procedure is summarised in the flowchart presented in Figure 2.

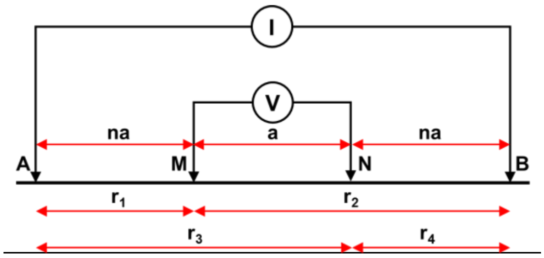

Figure 1. Schlumberger Configuration Electrode Arrangement [13]

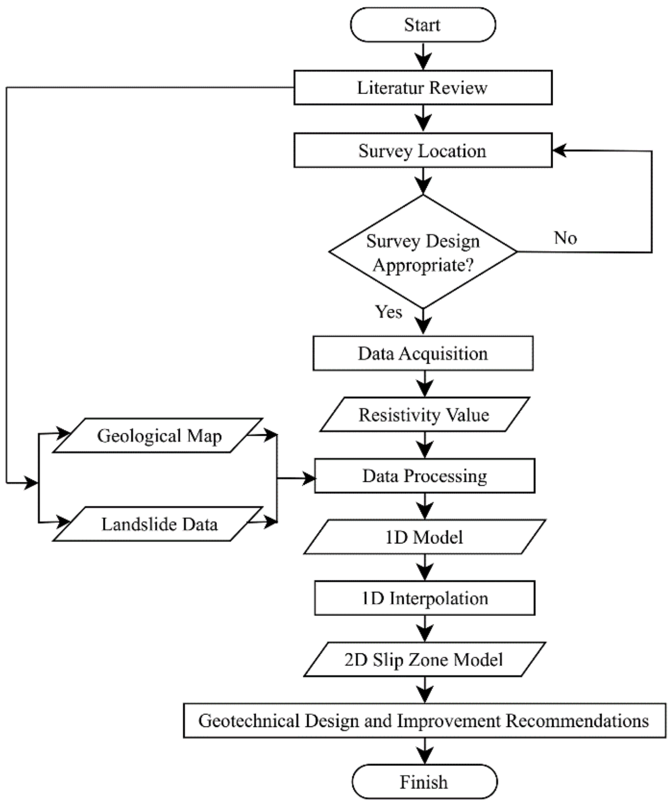

Figure 2. Research Flowchart

The data acquisition process employed the Schlumberger configuration of geoelectrical resistivity to investigate the vertical subsurface conditions of the soil. Eight measurement points were strategically distributed around the PT Molindo site, including the immediate landslide area (Figure 3), to assess the subsurface conditions comprehensively. PT Molindo is located in Lawang sub-district, Malang Regency, East Java Province, Indonesia. The primary objective of this investigation is to determine the depth and distribution of bedrock beneath the landslide-affected zone. Identifying the bedrock horizon is critical, as it serves as a reference point for designing and implementing geotechnical engineering interventions to stabilize the slope and mitigate further failures [21].

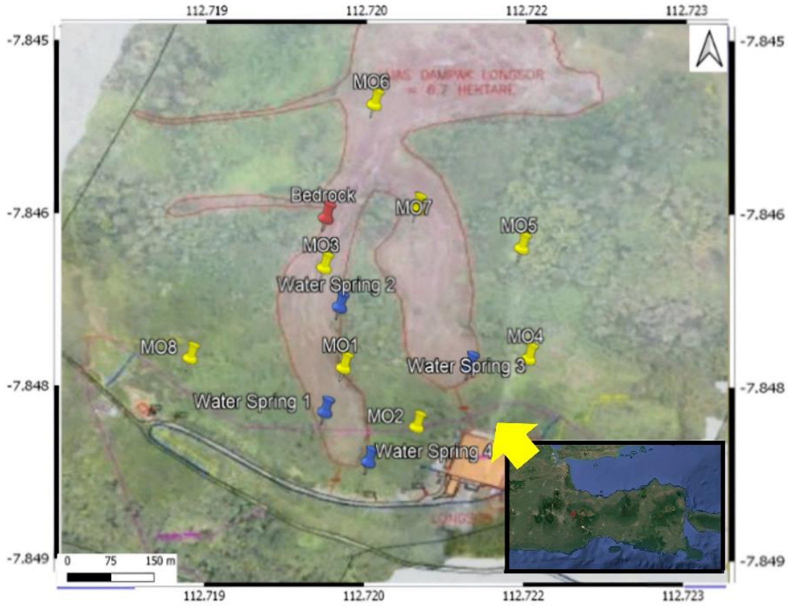

Figure 3. Research Survey Design

According to the Geological Map of the Malang Quadrangle (1992), the PT Molindo Lawang site is situated within the Lower Quaternary Volcanic Rock Formation, denoted as Qp(g) (Figure 4). This formation dates back to the Middle Pleistocene epoch and is primarily composed of volcanic breccia, tuff breccia, lava flows, tuff, and agglomerate [22]. Weathered materials, including clay-rich soils and organic-rich vegetation deposits, typically dominate the uppermost layers of this volcanic formation. At greater depths, lava serves as the bedrock. The interface between these superficial, unconsolidated layers and the underlying hard bedrock is particularly significant in geotechnical assessments. This contact zone often forms a mechanical discontinuity, which may act as a potential slip surface, especially under saturated conditions or in the presence of seismic or gravitational forces. The meeting of these two types of rock has the potential to produce a slip zone.

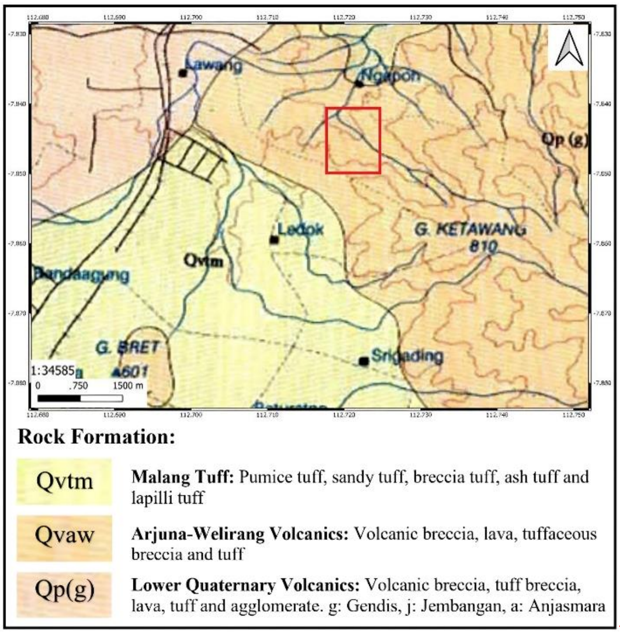

Figure 4. Geological Map of Malang Quadrangle [22]

2.2. Numerical Simulation Procedure

The steep slope conditions on the eastern and southern sides of the PT Molindo Lawang Incinerator Unit present a significant risk of landslides. Appropriate mitigation measures must be implemented based on the site's geological and topographical characteristics to address this. The soil and rock parameters used in the analysis are derived from previous research findings [23]. In this study, two slope stabilization alternatives are proposed. The first involves geometric reconfiguration of the slope and the installation of horizontal drainage to manage subsurface water flow. The second alternative integrates soil nailing reinforcement with geometric modification of the slope. To evaluate the effectiveness of both approaches, slope stability analyses are conducted using *Slope/W* software under static and dynamic conditions. Landslide occurrences in the area are suspected to be primarily triggered by the steep natural geomorphology and the absence of adequate drainage systems, which contribute to increased water infiltration and decreased soil shear strength.

3. Result and Discussion

3.1. Field Survey and Site Investigation

The landslide at PT Molindo occurred on March 8, 2022, and the failure process was relatively rapid, unfolding over approximately 3 to 6 hours (PT Molindo landslide incident history). Based on field observations, the landslide was classified as a rotational type, characterized by a curved slip surface. The displaced material primarily consisted of clay-rich soils and weathered claystone, with failure zones identified in two locations beneath the incinerator unit, extending to an estimated depth of 20 meters below the ground surface. The landslide body spans approximately 55 meters on the western and 75 meters on the eastern sides (Figure 5-a). The landslide characteristics in this area are similar to those of typical landslides. However, the area below the landslide location is a residential and agricultural area that serves as the primary source of livelihood for the local community, making immediate mitigation measures essential. The slope gradient at the study site ranges between 50° and 70°, classifying the area as steep terrain and highly susceptible to mass movement [24]. During the geoelectrical resistivity survey conducted on June 25–26, 2022, several active springs were observed near the landslide area (Figure 5-b and Figure 5-c). Significant groundwater discharge was recorded despite the survey during the dry season, indicating persistent subsurface flow. These springs are believed to originate near the interface between the clay layers and the underlying igneous bedrock. This lithological boundary is of particular concern, as the contrast in material properties can serve as a potential slip surface, promoting landslide initiation, especially under saturated conditions. Such groundwater flow at critical stratigraphic boundaries underscores the importance of effective drainage management in future mitigation efforts [25].

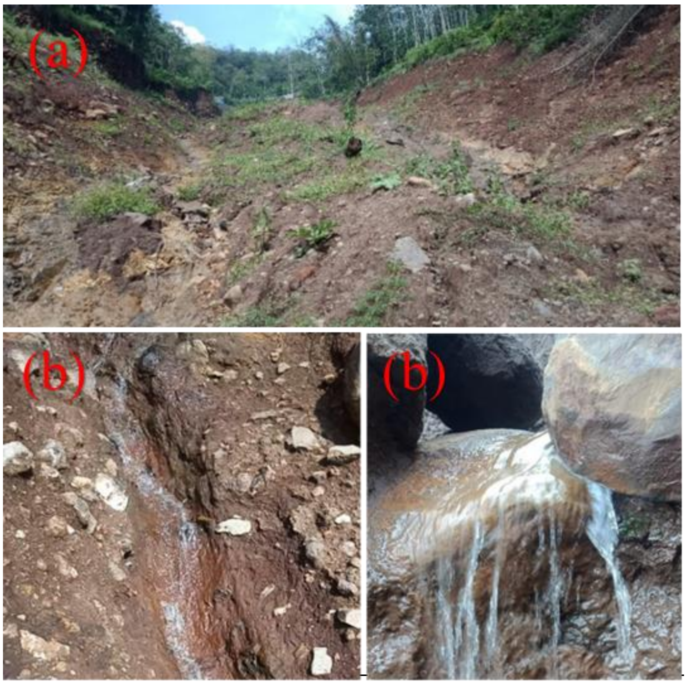

Figure 5. a. Landslide Conditions in the Research Area, b. Discovery of Water Flow at the Landslide Site

The highly steep terrain in the study area facilitates groundwater flow under considerable pressure, which can potentially mobilize soil and rock layers. During the dry season, however, the soil and rock mass can withstand this groundwater pressure, maintaining a state of equilibrium that prevents movement. The critical condition arises during the rainy season, when intense rainfall contributes to increased groundwater pressure through rainwater infiltration and surface runoff. The deteriorating condition of existing vegetation exacerbates this issue, as the reduced root reinforcement diminishes the soil's cohesion. Consequently, the cohesive strength (c), a key component of shear strength (τ) in the soil, declines, weakening the bond between soil and rock layers. This reduction in cohesive strength, combined with elevated pore water pressure (u) due to increased water infiltration, reduces the effective stress acting within the slope in both lateral and axial directions. Once pore pressure exceeds the soil's ability to resist deformation, the soil and rock layers lose their resistance to lateral or downslope movement. Impermeable layers, often between clay and bedrock, can be slip surfaces. These facilitate the downslope movement of overlying weathered soil under elevated groundwater pressure.

Impermeable layers act as a slip zone, allowing the overlying weathered soil to move along the slope direction with increasing groundwater pressure quickly. Increased water content or hydrostatic pressure can significantly trigger landslide mechanisms [26]. Landslide susceptibility is generally closely linked to soil characteristics and slope geometry. Steep terrain significantly increases landslide risk due to the inherently low stability of slope-forming materials [27]. At the PT Molindo site, slope gradients range from 50° to 70°, further intensifying the potential for slope failure [28]. The land use in the landslide-affected area consists of jungle-like vegetation with wild plant growth and scattered large trees growing irregularly. This lack of organized vegetation cover contributes to poor slope reinforcement. In addition to groundwater flow, the steep slope inclination is a significant factor contributing to landslide risk in this region [29]. Figure 6 presents a 3D topographic model of the study area, illustrating slope gradients and providing visual insight into the direction and position of potential landslide movements. The extent of the landslide zone is indicated in brown.

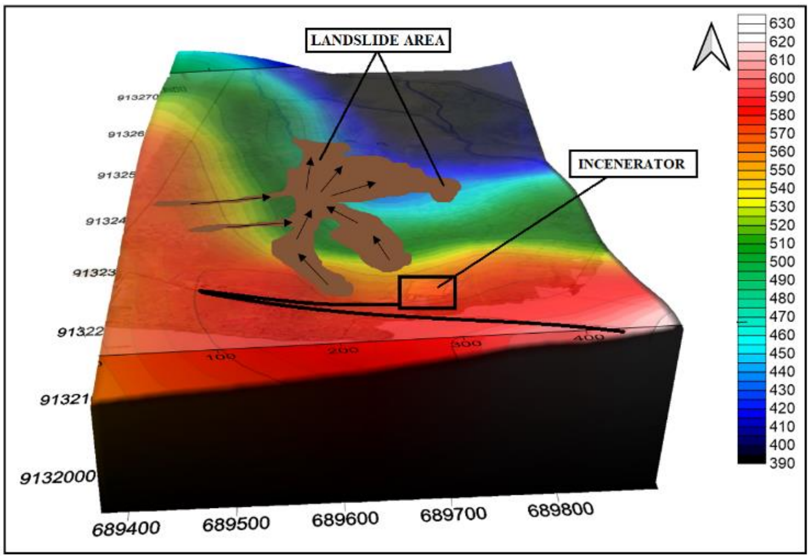

Figure 6. 3D Elevation Model

3.2. Resistivity Survey Result

The geoelectrical resistivity measurements using the Schlumberger configuration at eight measurement points were used to create a 1D model using IPI2Win and Progress software. IPI2win software can perform data picking and forward modeling of apparent resistivity data by matching field-derived curves with theoretical curves. After the data is prepared, inversion is then performed using the Progress software to obtain a one-dimensional resistivity profile. Based on the 1D model, the type of lithology composing the area can be analyzed based on the obtained resistivity values. Theoretically, the rock composition in the landslide area from field measurements is not significantly different from the geological map. The rocks include clay in the first layer, followed by sandy soil, with the bedrock consisting of lava rock.

Based on Figure 7, the geoelectrical resistivity survey yielded resistivity values ranging from 2.79 to 15.944 Ωm, with investigations reaching a maximum depth of approximately 48 meters below the ground surface. These values were interpreted using standard rock resistivity parameters to infer subsurface lithology. Clay-rich layers were identified at resistivity values between 3.30 and 25 Ωm, typically occurring at 0 to 32 meters depths. Sandy soil lithology was associated with intermediate resistivity values ranging from 26 to 167 Ωm, observed at depths between 2 and 21.4 meters. Bedrock, interpreted as lava rock, was characterized by high resistivity values ranging from 167 to 15.944 Ωm, found at depths of 17 to 48 meters across all survey profiles. Furthermore, indications of the groundwater table and zones of groundwater accumulation were observed at points MO4 and MO8. These were identified by very low resistivity values of 2.79 and 4.35 Ωm, located at depths between 4 and 7 meters. The presence of groundwater is very possible, because based on field observations, we found groundwater at the landslide location shown in Figure 5.

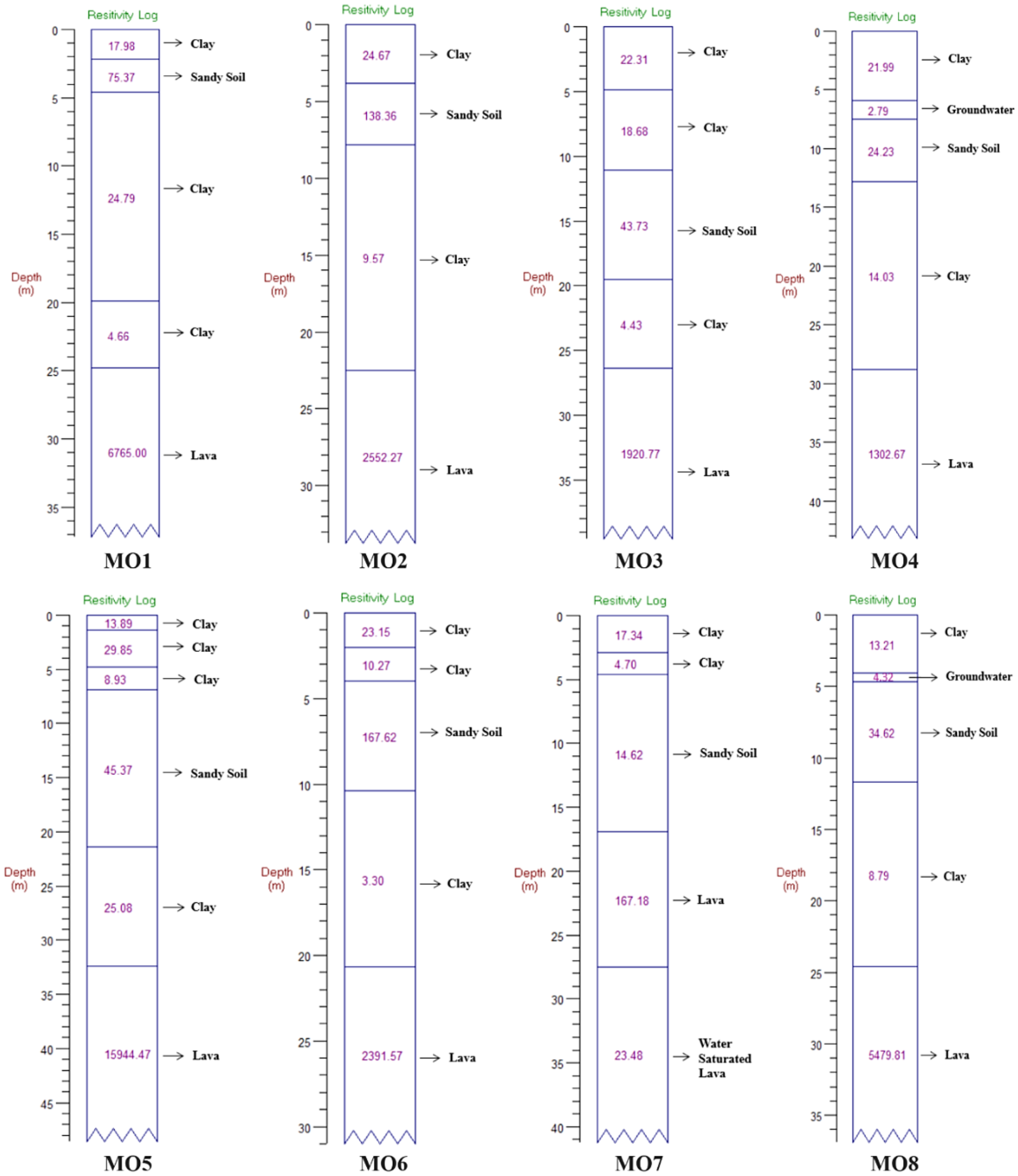

Figure 7. Results of 1D Model

The determination of layer types is based on the results of resistivity calculations, then correlated with resistivity value catalogues, local geological information, and relevant previous research, followed by further correlation with field conditions and geological theory. This process aims to obtain more accurate results. Based on the rock resistivity value catalogue compiled by Telford et al. (1990), clay has a resistivity value ranging from 1 to 100 Ωm, while sand from 1 to 1000 Ωm [30]. These range values represent the universal resistivity values of rock materials; therefore, to determine the actual values, it is necessary to consider the local geological conditions and the types of rocks in the research area.

Based on the modelling results, lava rocks that act as bedrock are always preceded by clay layers with low resistivity values, ranging from 3.30 to 25 Ωm. The interface between the clay and lava layers is interpreted as a slip zone, due to the significant differences in their physical and mechanical properties. This condition reinforces the indication that the slip zone is formed in the contact zone between an impermeable layer or compact rock and a layer that is easily deformed. This argument is supported by research from Hasan et al. (2022), which states that the contact between two layers with a significant difference in resistivity values can act as a sliding surface [13], such as the meeting between clay and lava rock. Research by Imani et al. (2021) also states that water infiltration can be trapped between the clay and bedrock layers, thereby increasing pore water pressure and reducing mechanical properties, ultimately causing mass movement [31], this means that the zone acts as a slip zone. In this research, the slip zone layer was found at varying depths at each measurement point, which is summarised in Table 1. The variation in bedrock depth is a common phenomenon because slope surfaces are generally not flat and experience elevation changes due to geomorphological processes.

Table 1. Summary of Slip Zones

Point	Depth of Slide Zone (m)	Resistivity Value (Ωm)
MO1	25	4.66
MO2	23	9.57
MO3	26	4.43
MO4	29	14.03
MO5	32	25.08
MO6	21	3.30
MO7	17	14.62
MO8	25	8.79

The one-dimensional (1D) resistivity models presented in Figure 7 were subsequently interpolated into two-dimensional (2D) profiles, as shown in Figure 8**,** to ensure the identification of potential slip zones at various depths. The contrast between subsurface lithologies, particularly the interface between clay-rich soils and compact lava rock, is critical in slope instability. While lava rock, interpreted as bedrock, typically remains stable due to its dense and compact nature, the overlying clay layers possess lower porosity and density. When these two contrasting materials intersect, water accumulates along the contact zone, forming an impermeable boundary that can act as a slip surface. Under increasing groundwater pressure, this condition enables the weathered overburden to mobilize downslope. Elevated water content or hydrostatic pressure is a well-known trigger for landslide initiation [26].

As illustrated in Figure 8 and Table 1, the potential slip zone is interpreted at an average depth of 20 to 25 meters, indicated by very low resistivity values (represented by purple colouring), with resistivity values between 3.30 and 25 Ωm. The clay observed on the ground surface is not a landslide trigger, so in this study, we do not classify it as a slip zone. This is because the surface clay tends to be dry, making it denser and difficult to deform. This condition is different from clay which is located directly adjacent to bedrock, this clay can become a place for groundwater accumulation. Groundwater in this zone significantly reduces the soil's cohesion (c) and internal friction angle (ϕ), both critical to maintaining slope stability. This interpretation aligns with field evidence, where landslide activity was observed at depths of 20–23 meters, demonstrating consistency between geophysical data and actual slope failure conditions. Further analysis based on Figure 7 reveals that the bedrock, identified as lava rock, was found starting at a depth of approximately 17 meters (MO7 point) below the surface. The overlying layers are predominantly clay and sandy soils prone to deformation and displacement. As such, any proposed stabilization measures, such as the installation of bored pile foundations, should be designed to penetrate to a minimum depth of 5 meters from the bedrock surface to ensure anchorage within the stable bedrock. This approach is essential for resisting movement in the more mobile overburden materials. Landslide susceptibility is strongly influenced by soil characteristics, with weak and weathered materials especially prone to failure. Steep slopes further exacerbate this instability due to the reduced inherent shear strength of the slope-forming materials [27].

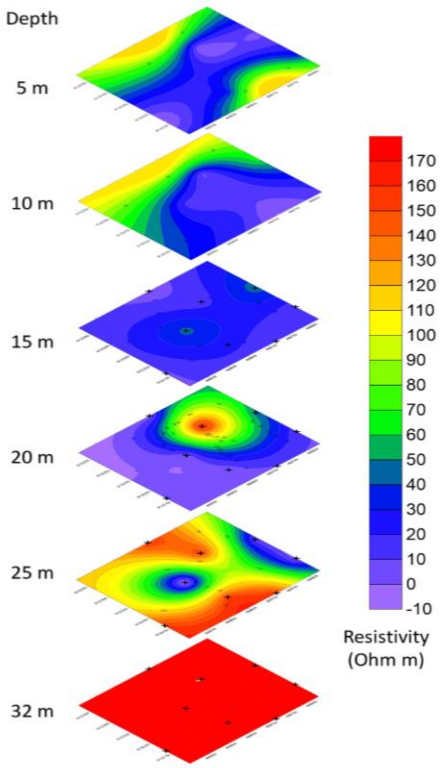

Figure 8. 2D Model of Research Area Showing Rock Resistivity Values with Depth Variation

Additionally, the presence of active groundwater sources contributes to slope failure by increasing the weight of the soil mass and elevating pore water pressure, both of which reduce effective stress and shear strength on the slope [32]. Effective stress declines rapidly when groundwater pressure surpasses the total soil stress, leading to slope movement. As pore pressure increases, soil, soil mixtures, and rock fragments are mobilized along the slope, with the additional weight of water compressing and weakening the soil structure, ultimately triggering surface deformation and landslide activity [33]. Therefore, the slope repair design must allow the water at the landslide location to flow freely, because if the water is retained, it will accumulate, ultimately triggering mass movement of the soil.

3.3. Recommendations for Improvement

Based on the integration of geological, topographic, and hydrological analyses, along with land cover assessments conducted through direct field observations, geoelectrical resistivity surveys, and geological mapping, and in consideration of the recent landslide events surrounding the PT Molindo Incinerator Unit, the following priority mitigation interventions are recommended:

3.3.1. Improving Drainage

Both surface and subsurface drainage improvements are essential, as water is the primary triggering factor in landslide initiation. Enhancing drainage systems in the catchment area surrounding the PT Molindo Incinerator Unit can significantly improve slope stability in landslide-prone zones (Figure 9). Effective water infiltration management, particularly on steep slopes, is critical to reducing the risk of slope failure [34]. Therefore, the presence and movement of groundwater within the landslide area must be carefully managed. It is imperative that any landslide mitigation structures, such as retaining walls or subsurface barriers, are designed not to obstruct the natural flow of groundwater. Blocking subsurface flow can lead to water accumulation, which increases the soil mass's weight and the hydrostatic pressure, ultimately elevating the risk of slope instability.

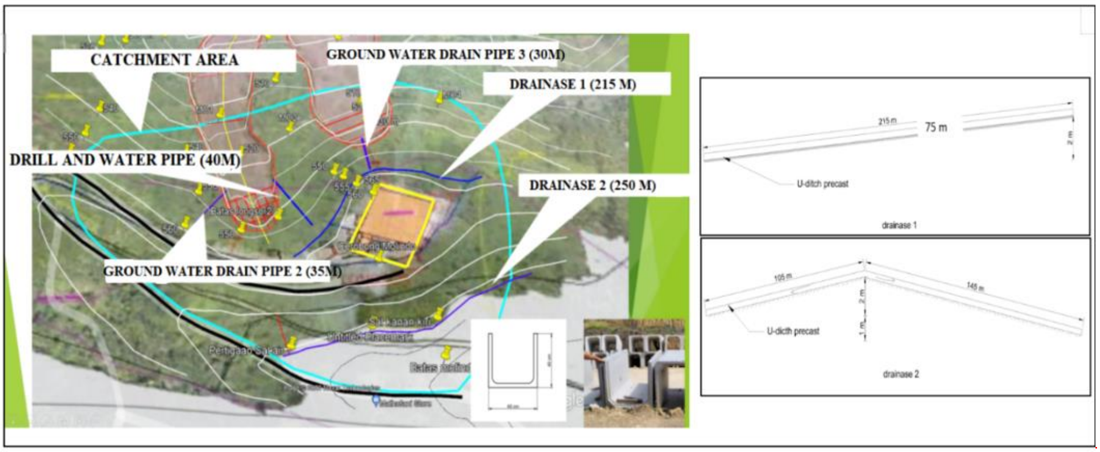

Figure 9. Drainage Design around the Landslide Area

Improvements to lateral and vertical drainage systems reduce pore water pressure (u) to near-zero levels, thereby maintaining the slope materials' shear strength (τ). Shear strength is defined by the equation $\tau = c + \sigma' \tan \varphi$, where c is soil cohesion, σ' is effective stress, and φ is the internal friction angle. Effective stress (σ') is calculated as the difference between total stress (σ_total) and pore water pressure (u). A properly functioning drainage system minimizes u, allowing σ' to approach σ_total. As a result, the soil retains its cohesion and internal friction parameters, maintaining overall slope stability. In this context, drainage plays a critical role in ensuring that increased water content does not compromise the mechanical strength of the soil or trigger landslide mechanisms. Cost estimation required for installing a drainage system on the upper surface of the slope in 2 (two) locations is around 10.919.61 USD or 180.075.300.00 IDR, using a precast U-Ditch of 30.50.120 cm in size with long of 215 and 250 m.

3.3.2. Construction of Retaining Wall

Retaining walls are commonly installed on steep slopes, riverbanks, and road edges. The purpose of constructing a retaining wall is to hold back loose materials from falling directly downward. Coarse-grained materials such as sand, gravel, and large stone fragments are typically used to retain walls and facilitate water drainage. The retaining wall's construction must reach the bedrock's depth to restrain soil movement effectively. Additionally, the presence of water in the landslide area must be preserved, meaning that the construction of landslide barriers should not obstruct groundwater flow (Figure 10). Cost estimation of a retaining wall which is made by a combination of concrete pile-gabions 68.35 m in size, close to 137.687.22 USD or 2.270.600.000.00 IDR.

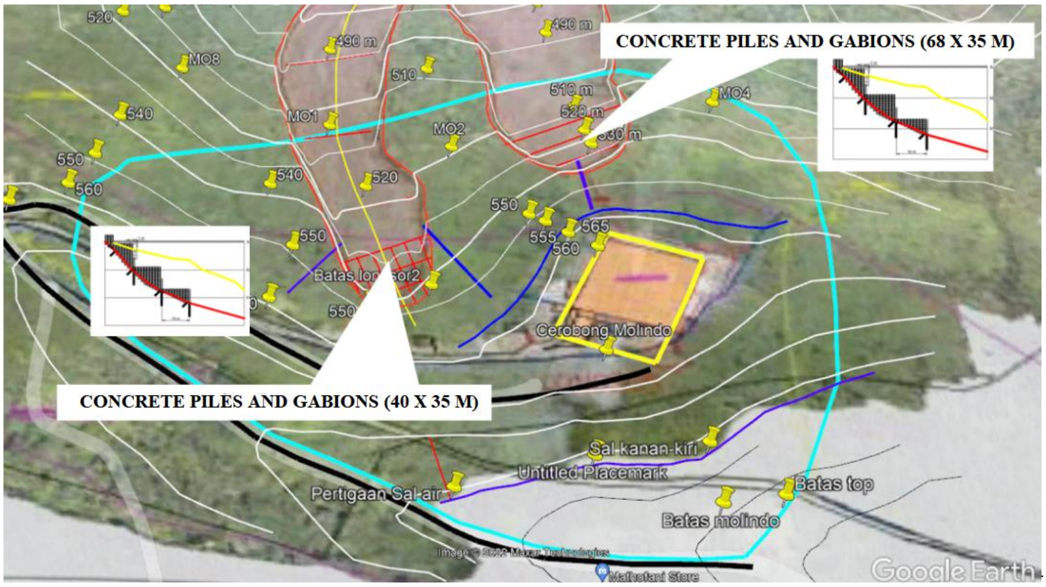

Figure 10. Retaining Wall Design at the Landslide Site

3.3.3. Soil Nailing Installation

The slope stability analysis before and after implementing a soil nailing system is presented in Figure 11. Based on Figure 11-a, the analysis results show that, under existing conditions, the safety factor ranges from 0.20 to 0.45 in static conditions and from 0.15 to 0.25 in dynamic conditions, indicating critically unstable slopes. Corresponding maximum deformations are estimated to be between 0.21 and 0.35 meters in static conditions and 0.82 to 1.15 meters in dynamic conditions. Following the installation of the soil nailing system, the slope demonstrates a significant improvement in stability (Figure 11-b). The safety factor increases to 1.31–1.81 under static conditions and 1.22–1.43 under dynamic conditions. Deformations are also substantially reduced, ranging from 0.01 to 0.02 meters in static and 0.02 to 0.03 meters in dynamic conditions. The effectiveness of soil nailing as a remedial measure can be further optimized by enhancing parameters such as pull-out resistance, nail diameter, and nail spacing, while also considering factors such as material availability, ease of implementation, cost-effectiveness, and long-term performance. Soil nailing is particularly advantageous for mitigating landslide risks on steep slopes during the rainy season, as it helps alter pore pressure distributions by redirecting subsurface flow toward the lower portions of the slope, thereby improving overall slope stability. The scope of soil nailing work includes gradient drilling and grouting, nailing installation, re-grouting and pulling out after bar installation, geo-composite using wire-mesh and shotcrete. Cost estimation of soil nailing for 68.35 m in length and 40.0 m in height, close to 134.550.41USD or 2.223.000.000.00 IDR.

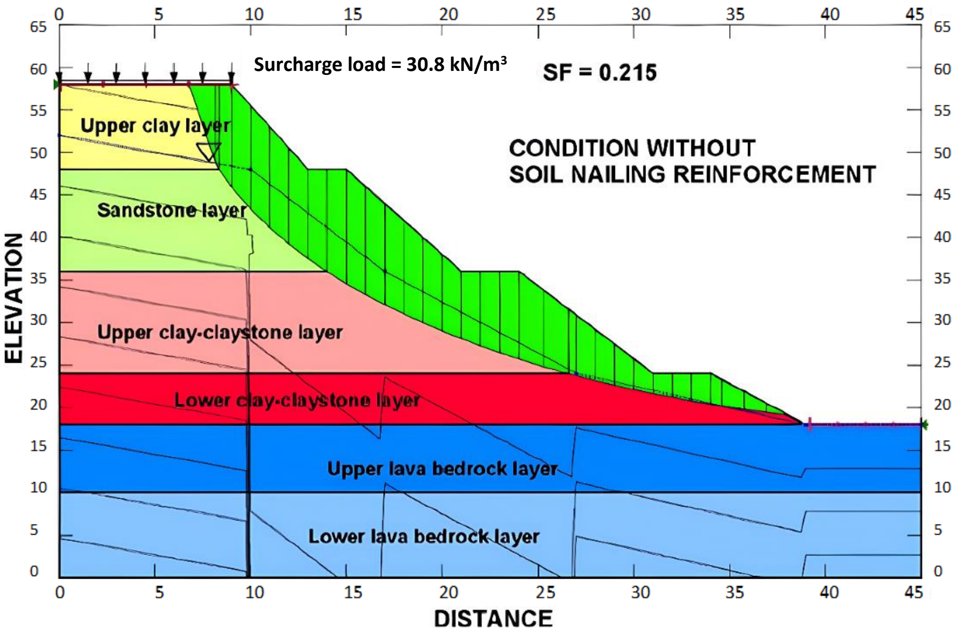

(a) Condition without soil nailing

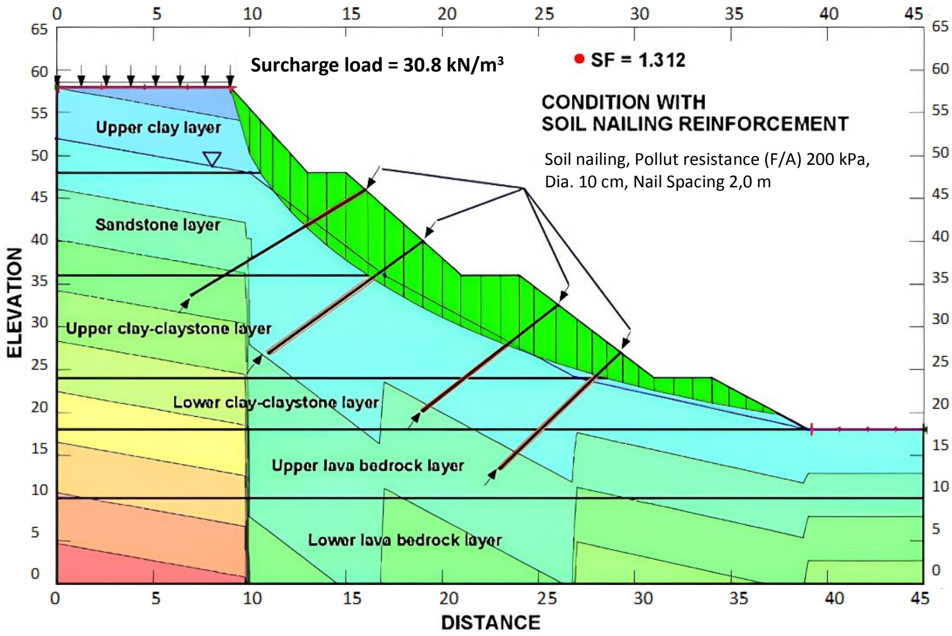

(b) Condition with soil nailing

Figure 11. Typical Analysis of Safety Factors Before and After Reinforcement

The compression stress of sandy soil, upper and lower clay-claystone layers, except the upper and lower lava bedrock layer, is more stable than the tensile stress [35, 36]. These tensile stresses will lead to the destabilization of soil and rock slopes. The reinforcement system of soil nailing will increase slope stability because the interaction between the soil or rock and soil nailing can lead to the development of tensile force. The stabilization process's starting point, including excavation for straightening the shape of the slope, can begin from the bottom since the upper and lower lava bedrock is stronger than the previous layers above. Various geotechnical activities and artificial contributions can increase the active force, creating a potential for soil and rock slope collapse. So, these problems can be improved by increasing the passive force using a soil nail system inserted into the slope. Then, the passive force will increase the shear resistance of soil and rock layers.

Composite stress between soil or rock with the soil nailing method can generate a resistance zone consisting of active and passive zones, as shown in Figure 11-b. Deformations caused by the active zones can lead to some displacements around the soil nailing system at a cross-section of the failure surface. However, the displacement formation of soil nailing resulting from tensile forces at a resistance zone will retain all active zones so that the failure surface can be stable. The deformation of soil nailing will depend on the length of the soil nailing system. There are essential things to consider in the area of the active and resistant zones to guarantee the stabilization of steep slopes and to avoid the failure of soil nailing

The effectiveness of the soil nailing system is influenced by several design parameters, particularly the length of the nails, which must adequately penetrate the passive zone to counteract forces in the active zone. The design should ensure sufficient overlap to stabilize the failure surface and avoid nail pull-out or structural failure. In addition, factors such as nail inclination, orientation, and the inclusion of helical plates can significantly influence the pull-out resistance and the system's overall performance under static and seismic conditions [37]. In soil nailing reinforcement systems, two critical types of analyses are required for calculating the factor of safety (SF): external stability analysis and internal stability analysis. The external stability analysis encompasses two key components. First, global stability analysis is conducted to evaluate the SF against large-scale slope failure, providing insight into the overall integrity of the reinforced slope system [38]. Second, displacement analysis assesses the SF related to potential sliding or deformation of the slope mass, considering axial and lateral forces that may result from surcharge loads or structural influences from above.

The internal stability analysis also involves two components. The first is a reinforcement bar failure analysis, which is used to determine the appropriate spacing and tensile strength of the soil nails and their ability to withstand soil pressures. The second is the pull-out capacity analysis, which evaluates the resistance of the reinforcement system to extraction forces. This is particularly important for preventing structural failure due to design flaws, such as insufficient nail length or embedment depth within the stable zone [39]. Various slip surface geometries—including parabolic and two-part wedge configurations—may be considered in modeling soil-nailed slopes. However, studies have shown that the variation in SF values between different slip surface shapes is generally minimal. Under seismic conditions, it is recommended to supplement the analysis with dynamic laboratory testing, such as cyclic triaxial tests, resonant column tests, and other forms of soil dynamics analysis. These tests are essential for determining the peak ground acceleration (PGA) and dynamic properties of the soil at the site, which are critical for reliable seismic slope stability design.

3.3.4. Vegetative Planting

Vegetation is an effective natural solution for increasing the stability of steep slopes, functioning both as slope cover and reinforcement through its root systems [40]. One of the key advantages of vegetation is its capacity for self-repair, regeneration, and adaptation, making it a low-maintenance, long-term strategy for slope stabilization. As vegetation adapts to its environment, its root systems develop in ways that integrate with the native soil, enhancing the root-soil interface and acting as a biological reinforcement system. In landslide-prone areas, vegetation can be established using a green belt planting method, where species are planted along contour lines or terraces at recommended intervals, such as 3 meters by 3 meters, aligned with land parcel boundaries This method allows the interspaces between planted rows for agricultural purposes, ensuring dual land use. Before planting, especially in high-risk areas, digging planting holes to support root establishment and reduce runoff is recommended. Integrating a soil nailing system with vegetative planting, such as vetiver grass, provides a synergistic reinforcement approach for slope stabilization in this study area [41]. The application of vetiver grass is widely regarded as an environmentally sustainable solution due to its deep, fibrous root system, which enhances surface soil cohesion and minimizes erosion. While the soil nailing system offers deep-seated structural support to prevent slope failure, the vetiver grass contributes to surface protection, mitigating erosion and reducing the impact of rainfall and surface runoff [42, 43].

Together, these methods form a complementary reinforcement system that addresses subsurface and surface instability, making it a practical and eco-friendly solution for landslide-prone slopes. In the short term, considerations such as access roads and proximity to highways should be addressed to ensure the success of trial plantings. When applied correctly, Vetiver grass can regenerate and anchor steep slopes within four to five years [44]. Vegetation can increase the slope's safety factor (SF); however, its effectiveness may be limited on slopes with large inclinations, where weak soil–root interactions can reduce reinforcement capacity. If the lateral root anchorage is insufficient, slope failure will likely occur when the SF falls below 1.0, indicating instability. While root systems typically improve slope safety by increasing cohesion and anchorage, the overall benefit depends on the underlying soil type and slope geometry. The success of vegetation-based reinforcement also depends on root penetration depth. Deep-rooted species can slightly increase the SF in clayey soils due to better resistance to deep-seated failure. Conversely, sandy soils often present challenges for vegetative growth due to their instability and reduced cohesion, particularly under external disturbances such as wind or animal activity [45]. In such cases, vegetation alone may not be sufficient, but when combined with soil nailing systems, it can effectively reduce landslide risk with appropriate maintenance [46].

Root systems enhance shear strength by contributing additional cohesion to the soil matrix. The overall stability of vegetated slopes tends to increase with greater root cohesion values and the development of an effective root zone depth**.** These effects are more pronounced on slopes where vegetation covers the surface and crest areas. The success of vegetative reinforcement also depends on the distribution pattern of the root system, which influences how shear stresses are transferred and resisted across the slope [47, 48]. Estimation for vegetative planting will be added by the green belt from grass vetiver plants, which ranges from 5.841.37 USD or 96.330.000.00 IDR.

4. Conclusion

The rock composition at the study site, encompassing the PT Molindo Incinerator Unit and its surrounding area, predominantly comprises claystone, sandy soil, and lava rock. Landslide materials observed at the site primarily consist of clay-rich deposits, identified in two separate zones beneath the incinerator at approximately 20 meters from the ground surface. The underlying bedrock, interpreted as volcanic lava, is consistently encountered at depths ranging from 17 to 32 meters. The potential slip zone is interpreted at an average depth of 20 to 25 meters, indicated by very low resistivity values (represented by purple colouring), with resistivity values between 3.30 and 25 Ωm. Given this subsurface profile, the design of foundations or retaining walls for effective landslide mitigation should extend to a minimum depth of 5 meters from the bedrock surface, ensuring structural anchorage within the stable bedrock layer to restrain soil movement comprehensively. In addition to structural considerations, active groundwater sources must be accounted for in the slope stabilization design. The natural emergence of springs and seepage pathways should not be obstructed, as impeding groundwater flow can lead to water accumulation, increased pore water pressure, and subsequent slope instability. Therefore, the design of land improvement and stabilization measures must accommodate and direct groundwater flow, incorporating drainage pathways that maintain hydrological balance while stabilizing the slope.

The proposed landslide mitigation strategy comprises several key interventions: (1) improvement of surface and subsurface drainage systems, (2) construction of retaining walls, (3) installation of soil nailing systems, and (4) implementation of vegetative planting. Numerical modeling using *Slope/W* software demonstrates that soil nailing significantly enhances slope stability, yielding safety factors between 1.32 and 1.81 under static conditions and 1.22 to 1.43 under dynamic conditions. The deformations are relatively minimal, ranging from 0.01 to 0.02 meters (static) and 0.02 to 0.03 meters (dynamic), indicating the system's effectiveness. The performance of the soil nailing system can be further optimized by adjusting design parameters such as pull-out resistance, nail diameter, and nail spacing. These adjustments should be made in consideration of material availability, ease of construction, cost-efficiency, and long-term durability, ensuring that the remedial measures are both technically and economically viable over the lifespan of the slope stabilization system.

5. Declarations

5.1. Author Contributions

Conceptualization, M.F.R.H. and A.S.; methodology, A.S., M.F.R.H., and A.T.S.H.; software, P.A.M.A., E.A.S., and M.H.I.; validation, A.S., E.A.S., and B.M.; formal analysis, M.F.R.H., P.A.M.A., and B.M.; investigation, A.S., M.F.R.H., A.T.S.H., and M.H.I.; resources, A.S. and A.T.S.H.; data curation, E.A.S., P.A.M.A., and B.M.; writing—original draft preparation, M.F.R.H. and M.H.I.; writing—review and editing, A.S., E.A.S., and B.M.; visualization, P.A.M.A. and M.H.I.; supervision, A.S.; project administration, A.T.S.H. and M.H.I. All authors have read and agreed to the published version of the manuscript.

5.2. Data Availability Statement

The data presented in this study are available on request from the corresponding author.

5.3. Funding

The authors received no financial support for the research, authorship, and/or publication of this article.

5.4. Acknowledgements

We express our gratitude to PT Molindo Lawang, Indonesia and Universitas Brawijaya for allowing the research team to address the landslide issues surrounding the Incinerator Unit area.

5.5. Conflicts of Interest

The authors declare no conflict of interest.

6. References

[1] Shanmugam, G., & Wang, Y. (2015). The landslide problem. Journal of Palaeogeography, 4(2), 109–166. doi:10.3724/SP.J.1261.2015.00071.

[2] Boyd, J. P., Binley, A., Wilkinson, P., Holmes, J., Bruce, E., & Chambers, J. (2024). Practical considerations for using petrophysics and geoelectrical methods on clay rich landslides. Engineering Geology, 334, 107506. doi:10.1016/j.enggeo.2024.107506.

[3] Ghiasi, V., Pauzi, N. I. M., Karimi, S., & Yousefi, M. (2023). Landslide risk zoning using support vector machine algorithm. Geomechanics and Engineering, 34(3), 267–284. doi:10.12989/gae.2023.34.3.267.

[4] Susilo, A., Juwono, A. M., Aprilia, F., Hisyam, F., Rohmah, S., & Hasan, M. F. R. (2023). Subsurface Analysis Using Microtremor and Resistivity to Determine Soil Vulnerability and Discovery of New Local Fault. Civil Engineering Journal (Iran), 9(9), 2286–2299. doi:10.28991/CEJ-2023-09-09-014.

[5] BPBD Malang Regency. (2022). Data Kejadian Bencana Kabupaten Malang (Data on Disaster Events in Malang Regency). Regional Disaster Management Agency (BPBD), Malang Regency Government, Jakarta, Indonesia.

[6] Hasan, M. F. R., Susilo, A., Suryo, E. A., Agung, P. A. M., Wiyono, Pratiwie, D. L., & Dewi, N. M. (2024). Assessment and simulation of potential landslide caused by the rainfall intensity in Batu City during 2021. IOP Conference Series: Earth and Environmental Science, 1314(1), 12017. doi:10.1088/1755-1315/1314/1/012017.

[7] Ering, P., & Babu, G. L. S. (2016). Probabilistic back analysis of rainfall induced landslide- A case study of Malin landslide, India. Engineering Geology, 208, 154–164. doi:10.1016/j.enggeo.2016.05.002.

[8] Mickus, K., Frifita, N., Ben Zaied, M., & Ouessar, M. (2022). Gravity and electrical resistivity analysis of deep and shallow structures related to aquifers within the Jeffara Plain, southeast Tunisia. Journal of African Earth Sciences, 196, 104685. doi:10.1016/j.jafrearsci.2022.104685.

[9] Pun, W. K., Chung, P. W. K., Wong, T. K. C., Lam, H. W. K., & Wong, L. A. (2020). Landslide Risk Management in Hong Kong - Experience in the Past and Planning for the Future. Landslides, 17(1), 243–247. doi:10.1007/s10346-019-01291-8.

[10] Luat, N. V., Do, T. N., Nguyen, L. C., & Kien, N. T. (2024). Assessing landslide susceptibility along the Halong – Vandon expressway in Quang Ninh province, Vietnam: A comprehensive approach integrating GIS and various methods. Geomechanics and Engineering, 37(2), 135–147. doi:10.12989/gae.2024.37.2.135.

[11] Yunita, F. T., Soekarno, I., Nugroho, J., & Santosa, U. B. (2024). Empirical Model of Unconsolidated Tephra Erosion: Verification and Application on Micro Catchment. Civil Engineering Journal, 10(7), 2088-2104. doi:10.28991/CEJ-2024-010-07-02.

[12] Whiteley, J. S., Watlet, A., Uhlemann, S., Wilkinson, P., Boyd, J. P., Jordan, C., Kendall, J. M., & Chambers, J. E. (2021). Rapid characterisation of landslide heterogeneity using unsupervised classification of electrical resistivity and seismic refraction surveys. Engineering Geology, 290, 106189. doi:10.1016/j.enggeo.2021.106189.

[13] Hasan, M. F. R., Salimah, A., Susilo, A., Rahmat, A., Nurtanto, M., & Martina, N. (2022). Identification of Landslide Area Using Geoelectrical Resistivity Method as Disaster Mitigation Strategy. International Journal on Advanced Science, Engineering and Information Technology, 12(4), 1484–1490. doi:10.18517/ijaseit.12.4.14694.

[14] Chaiyaput, S., Suksawat, T., Mase, L. Z., Sugiyama, M., & Ayawanna, J. (2023). The thickness of the soft soil layer and canal-side road failure: A case study in Phra Nakhon Si Ayutthaya province, Thailand. Geomechanics and Engineering, 35(5), 511–523. doi:10.12989/gae.2023.35.5.511.

[15] Di Maio, R., Salone, R., De Paola, C., Carbonari, R., Cusano, D., & De Vita, P. (2024). Geotechnical and geophysical property models of soil-covered slopes prone to landsliding. The case study of the Ischia Island (southern Italy). Catena, 247, 108509. doi:10.1016/j.catena.2024.108509.

[16] Hasan, M. F. R., Susilo, A., Suryo, E. A., Agung, P. A. M., Pratama, A., Idmi, M. H., & Mustaffa, A. A. (2024). The use of geoelectrical resistivity methods to detect the potential landslides in Payung, Batu City, Indonesia. IOP Conference Series: Earth and Environmental Science, 1347(1), 12003. doi:10.1088/1755-1315/1347/1/012003.

[17] Sujitapan, C., Kendall, J. M., Chambers, J. E., & Yordkayhun, S. (2024). Landslide assessment through integrated geoelectrical and seismic methods: A case study in Thungsong site, southern Thailand. Heliyon, 10(2), 24660. doi:10.1016/j.heliyon.2024.e24660.

[18] Hasan, M. F. R., Adi, S., & Sunaryo. (2018). Identification of underground river flow pattern using self-potential (SP) and resistivity methods for drought mitigation at Druju, Sumbermanjing Wetan, Indonesia. Disaster Advances, 11(5), 25–31.

[19] Hasan, M. F. R., Pradiptiya, A., Setiawan, Y., Agung, P. A. M., Susilo, A., & Sunaryo. (2022). Detection of groundwater sources in Lembor village using geoelectrical resistivity method schlumberger configuration. IOP Conference Series: Earth and Environmental Science, 1116(1), 12051. doi:10.1088/1755-1315/1116/1/012051.

[20] Sunaryo, Susilo, A., Yuwono, A. M., & Wiyono, W. (2019). Slope Stability Analysis for Landslides Natural Disaster Mitigation by Means of Geoelectrical Resistivity Data in Gedangan of South Malang, East Java, Indonesia. IOP Conference Series: Materials Science and Engineering, 546(2), 22030. doi:10.1088/1757-899X/546/2/022030.

[21] Arya, I. W., Wiraga, I. W., & Suryanegara, I. G. A. G. (2018). Effect of cement injection on sandy soil slope stability, case study: Slope in Petang district, Badung regency. Journal of Physics: Conference Series, 953(1), 12103. doi:10.1088/1742-6596/953/1/012103.

[22] Santosa, S., & Atmawinata, S. (1992). Geological Map of The Kediri Quadrangle, Jawa. Geological Research and Development Centre, Bandung, Indonesia.

[23] Liu, Y., Xiao, H., Yao, K., Hu, J., & Wei, H. (2018). Rock-soil slope stability analysis by two-phase random media and finite elements. Geoscience Frontiers, 9(6), 1649–1655. doi:10.1016/j.gsf.2017.10.007.

[24] Çellek, S. (2020). Effect of the Slope Angle and Its Classification on Landslide. Copernicus GmbH (Preprint), 1-23. doi:10.5194/nhess-2020-87.

[25] Marino, P., Comegna, L., Damiano, E., Olivares, L., & Greco, R. (2020). Monitoring the hydrological balance of a landslide-prone slope covered by pyroclastic deposits over limestone fractured bedrock. Water (Switzerland), 12(12), 3309. doi:10.3390/w12123309.

[26] Ling, C., Xu, Q., Zhang, Q., Ran, J., & Lv, H. (2016). Application of electrical resistivity tomography for investigating the internal structure of a translational landslide and characterizing its groundwater circulation (Kualiangzi landslide, Southwest China). Journal of Applied Geophysics, 131, 154–162. doi:10.1016/j.jappgeo.2016.06.003.

[27] Bachri, S., Shrestha, R. P., Yulianto, F., Sumarmi, S., Utomo, K. S. B., & Aldianto, Y. E. (2021). Mapping landform and landslide susceptibility using remote sensing, GIS and field observation in the Southern Cross road, Malang regency, East Java, Indonesia. Geosciences (Switzerland), 11(1), 1–15. doi:10.3390/geosciences11010004.

[28] Azarafza, M., Nanehkaran, Y. A., Rajabion, L., Akgün, H., Rahnamarad, J., Derakhshani, R., & Raoof, A. (2020). Application of the modified Q-slope classification system for sedimentary rock slope stability assessment in Iran. Engineering Geology, 264, 105349. doi:10.1016/j.enggeo.2019.105349.

[29] Castro, J., Asta, M. P., Galve, J. P., & Azañón, J. M. (2020). Formation of clay-rich layers at the slip surface of slope instabilities: The role of groundwater. Water (Switzerland), 12(9), 2639. doi:10.3390/w12092639.

[30] Telford, W. M., Geldart, L. P., & Sheriff, R. E. (1990). Applied Geophysics. Cambridge University Press, Cambridge, United Kingdom. doi:10.1017/cbo9781139167932.

[31] Imani, P., Tian, G., Hadiloo, S., & El-Raouf, A. A. (2021). Application of combined electrical resistivity tomography (ERT) and seismic refraction tomography (SRT) methods to investigate Xiaoshan District landslide site: Hangzhou, China. Journal of Applied Geophysics, 184, 104236. doi:10.1016/j.jappgeo.2020.104236.

[32] Uhlemann, S., Chambers, J., Wilkinson, P., Maurer, H., Merritt, A., Meldrum, P., Kuras, O., Gunn, D., Smith, A., & Dijkstra, T. (2017). Four-dimensional imaging of moisture dynamics during landslide reactivation. Journal of Geophysical Research: Earth Surface, 122(1), 398–418. doi:10.1002/2016JF003983.

[33] Wicki, A., Lehmann, P., Hauck, C., & Stähli, M. (2023). Impact of topography on in situ soil wetness measurements for regional landslide early warning - a case study from the Swiss Alpine Foreland. Natural Hazards and Earth System Sciences, 23(3), 1059–1077. doi:10.5194/nhess-23-1059-2023.

[34] Hasan, M. F. R., Agung, P. A. M., Susilo, A., Suryo, E. A., Zainorabidin, A. Bin, & Hermawan, A. R. (2024). Wedge Slope Failure of Natural Sedimentary Rock Formation Based on Weathering Potential. International Journal of Design and Nature and Ecodynamics, 19(2), 387–396. doi:10.18280/ijdne.190204.

[35] Rout, S. K., De, M., Mandal, A. K., & Das, B. (2019). Soil Nailing for Failed Slope Stabilization on Hilly Terrain. Geotechnics for Transportation Infrastructure. Lecture Notes in Civil Engineering , 28, Springer, Singapore. doi:10.1007/978-981-13-6701-4_40.

[36] Pandey, A., Jaiswal, S., & Chauhan, V. B. (2021). Numerical Studies on the Behavior of Slope Reinforced with Soil NailsLocal Site Effects and Ground Failures. Lecture Notes in Civil Engineering, Springer, Singapore. doi:10.1007/978-981-15-9984-2_19.

[37] Dewedree, S., & Jusoh, S. N. (2019). Slope stability analysis under different soil nailing parameters using the SLOPE/W software. Journal of Physics: Conference Series, 1174(1), 12008. doi:10.1088/1742-6596/1174/1/012008.

[38] Villalobos, S. A., & Villalobos, F. A. (2021). Effect of nail spacing on the global stability of soil nailed walls using limit equilibrium and finite element methods. Transportation Geotechnics, 26, 100454. doi:10.1016/j.trgeo.2020.100454.

[39] Mohamed, M. H., Ahmed, M., & Mallick, J. (2021). Pullout behavior of nail reinforcement in nailed soil slope. Applied Sciences (Switzerland), 11(14), 6419. doi:10.3390/app11146419.

[40] Teshale, E., & Legesse, A. (2022). The Effects of Vetiver Grass (Vetiver Zizanodes L.) on Soil Fertility Enhancement, Soil Water Conservation, Carbon Sequestration and Essential oil Productions A: Review. Journal of Natural Sciences Research, 8(1), 25–31. doi:10.7176/jnsr/13-5-04.

[41] Ma, S., Xu, C., Xu, X., He, X., Qian, H., Jiao, Q., Gao, W., Yang, H., Cui, Y., Zhang, P., Li, K., Mo, H., Liu, J., & Liu, X. (2020). Characteristics and causes of the landslide on July 23, 2019 in Shuicheng, Guizhou Province, China. Landslides, 17(6), 1441–1452. doi:10.1007/s10346-020-01374-x.

[42] Mahmoudpour, M., Gholami, S., Ehteshami, M., & Salari, M. (2021). Evaluation of Phytoremediation Potential of Vetiver Grass (Chrysopogon zizanioides (L.) Roberty) for Wastewater Treatment. Advances in Materials Science and Engineering, 3059983. doi:10.1155/2021/3059983.

[43] Liu, X., Lan, H., Li, L., & Cui, P. (2022). An ecological indicator system for shallow landslide analysis. Catena, 214, 106211. doi:10.1016/j.catena.2022.106211.

[44] Nghia, N. T., Lam, L. G., & Hino, T. (2019). Combining soil nail and vetiver grass in a slope protection project in Vietnam. Lowland Technology International, 21(1), 14–22.

[45] Lavania, S. (2019). Vetiver grass model and phenomics of root system architecture. The Journal of Indian Botanical Society, 98(3and4), 176. doi:10.5958/2455-7218.2019.00020.2.

[46] Nguyen, B. T., Ishikawa, T., & Murakami, T. (2020). Effects evaluation of grass age on hydraulic properties of coarse-grained soil. Transportation Geotechnics, 25, 100401. doi:10.1016/j.trgeo.2020.100401.

[47] Sittadewi, E. H., & Tejakusuma, I. G. (2019). the Role of Root Plant Architecture in Landslide and Erosion Disaster Mitigation. Jurnal Sains Dan Teknologi Mitigasi Bencana, 14(1), 54–61. doi:10.29122/jstmb.v14i1.3552.

[48] Tsige, D., Senadheera, S., & Talema, A. (2019). Stability Analysis of Plant-Root-Reinforced Shallow Slopes along Mountainous Road Corridors Based on Numerical Modeling. Geosciences, 10(1), 19. doi:10.3390/geosciences10010019.

[49] Zhang, L., Li, M., & Zhao, B. (2018). Experimental Study on Tensile Properties and Reinforcement Ability of Plant Roots. Nature Environment & Pollution Technology, 17(3), 729-738.